THE ANATOMICAL RECORD PART A 278A:505–513 (2004)

Ultrastructure of the Osteocyte Process and its Pericellular Matrix

LI-DAN YOU,[1] SHELDON WEINBAUM,[1] STEPHEN C. COWIN,[1] AND MITCHELL B. SCHAFFLER[2]*

[1]Center for Biomedical Engineering, Department of Mechanical Engineering, City College of New York, New York, New York

[2]Leni and Peter W. May Department of Orthopaedics, Mount Sinai School of Medicine, New York, New York

ABSTRACT

Osteocytes are believed to be the mechanical sensor cells in bone. One potential physical mechanism for the mechanosensing process is that osteocytes directly sense the deformation of the substrate to which they are attached. However, there is a fundamental paradox in this theory: tissue-level strains in whole bone are typically $<0.2\%$, yet an extensive range of in vitro experiments show that dynamic substrate strains must be at least an order of magnitude larger in order for intracellular biochemical responses to occur. Recently, a theoretical model was developed (You et al. J. Biomech., 2001; 34:1375–1386) that provides a possible mechanism by which mechanical loading-induced fluid flow in the lacuno-canalicular system, under routine physical activity, can produce cellular-level strains on the osteocyte processes that are at least one order of magnitude larger than bone tissue deformations. This would resolve the fundamental paradox mentioned above. In this work we experimentally confirm and quantify the essential ultrastructural elements in this model: 1) the presence of the transverse elements that bridge the pericellular space surrounding the osteocyte process, which interact with the fluid flow and lead to an outward hoop tension on the process; and 2) the presence of bundled F-actin in the osteocyte processes, which resists the outward hoop tension and limits the cell process membrane deformation. Morphological data to support these assumptions are scant. Special staining techniques employing ruthenium III hexamine trichloride (RHT) were developed to elucidate these structures in the humeri of adult mice. Anat Rec Part A 278A:505–513, 2004.

Key words: osteocyte; transverse element; actin bundle; pericellular space; pericellular matrix

Bone is a biological system that continuously adjusts its structure to adapt to its mechanical environment. Mechanical signals are critical for this adaptation process. There are three types of bone cells: osteoblasts, osteocytes, and osteoclasts. The osteocytes are believed to be the cells that sense the mechanical load. These cells are embedded in the bone matrix and are connected to each other by slender cell processes located within the small bony tubes of the canaliculi.

Although osteocytes are believed to be the mechanosensor, it remains unknown how the mechanical load is transduced from the bone tissue to these cells. Some investigators have suggested that osteocytes sense whole tissue strains. However, this view leads to a fundamental paradox: the strains applied to whole bone (i.e., tissue-level strains) in vivo are much smaller (0.04–0.3%) (Rubin and Lanyon, 1984; Fritton et al., 2000) than the strains (1–10%) (You et al., 2000) that are necessary to activate bone cell signaling in cell cultures.

Recently, You et al. (2001) proposed a new strain amplification process and model to explain how mechanical loading-induced fluid flow in the lacuno-canalicular system, under routine physical activity, can produce deformations of osteocyte processes that are at least one order of magnitude larger than whole bone tissue deformations. This new model provides a plausible explanation for the

Grant sponsor: NIH; Grant numbers: AR48699; AR41210.

*Correspondence to: Mitchell B. Schaffler, Ph.D., Leni and Peter W. May Department of Orthopaedics, Mount Sinai School of Medicine, Box 1188, One Gustave L. Levy Place, New York, NY 10029. Fax: 212-426-7750. E-mail: mitchell.schaffler@mssm.edu

Received 10 November 2003; Accepted 14 March 2004

DOI 10.1002/ar.a.20050

discrepancy in the fact that the larger strains needed to stimulate bone cells cannot be derived from direct bone matrix deformation, since they would cause bone fracture. Briefly, the model assumes the existence of three basic components: 1) an organic matrix that fills the entire pericellular space surrounding the osteocyte body and the osteocytic processes, 2) transverse elements that anchor and center the osteocytic process within its canaliculus, and 3) a cytoskeletal structure within the cell processes that resists hoop tension and bending deformation. When bone is loaded, fluid flow is induced in the pericellular space of the lacuno-canalicular system in response to the deformation-induced pressure gradient (Piekarski and Munro, 1977; Weinbaum et al., 1994; Cowin et al., 1995; Knothe Tate et al., 1998; Knothe Tate and Knothe, 2000). You et al. (2001) proposed that the fluid drag on the pericellular matrix is transmitted to the transverse tethering elements in the pericellular space surrounding the osteocytic process, which causes the elements to deform in the shape of a catenary curve if the loading is uniform. This produces a tensile force that is transmitted to the cell process cytoskeleton by membrane-spanning proteins and linker molecules that generate an outward hoop strain on the osteocytic process membrane and the underlying cytoskeleton. The actin filament bundle in the osteocyte process provides the major resistance to this hoop strain. The balance of these two forces was shown by You et al. (2001) to result in a deformation of the cell cytoskeleton that is at least one order of magnitude larger than tissue-level strain. Hence, the osteocyte can be subjected to significant local mechanical loading through this coupling mechanism even though the tissue-level strain is very small.

Several anatomical parameter values for the osteocytic process, pericellular matrix, and canalicular structure are required in the model. These include the dimensions of the osteocytic process and canaliculus, the dimensions of the spacing between the transverse tethering elements, the spacing between the axial actin filaments, and the spacing of their cross-links. These structural components and their parameter values are critical for the validity of the model and its quantitative predictions. It is the very existence of these cell and matrix structures and their parametric values that motivated the current study.

While a number of experimental studies have investigated various aspects of the ultrastructure of osteocytes and their pericellular space (Weinger and Holtrop, 1974; Holtrop, 1975; King and Holtrop, 1975; Sauren et al., 1992; Shapiro et al., 1995; Bentolila et al., 1998), most of these have provided (at best) unclear or (at worst) contradictory information about the intimate relationship between the cell and its surrounding matrix, which is a key issue in resolving the paradox of mechanical stimulation outlined above. For example, even the fundamental question regarding the existence of a pericellular space, a space that is essential for all fluid flow-based theories of lacunocanalicular transport and mechanotransduction, remains unanswered. Almost all of these previous studies were performed on recently formed osteocytes in tissue from very young animals. It is not known whether osteocytes in mature bone have the same cytoskeletal and pericellular matrix structure as found in immature bone. The current studies were designed to investigate the ultrastructure of *mature* bone samples to 1) verify the existence of the pericellular space and its matrix contents in the fluid annulus surrounding the cell process, and quantify its dimensions; 2) investigate the existence of the transverse tethering elements in the pericellular matrix; 3) examine the axial microfilaments inside the osteocyte cell processes, and obtain initial estimates of their number density and spacing; 4) quantify the cell process and canalicular diameters; and 5) quantify the spacing between transverse elements in the pericellular matrix, and the spacing between the actin filaments in the process. The measurements for goals 4 and 5 will provide critical input data regarding osteocyte ultrastructure that are important for obtaining realistic quantitative predictions using the theoretical model described by You et al. (2001). These data are also important input for all theoretical models examining interstitial fluid flow in the lacuno-canalicular porosity in bone.

MATERIALS AND METHODS

Studies were performed on the humeri of 15-week-old BalB/cByJ female mice (n = 3, weight = 21–24 g). The diaphysis was cut into 1-mm-thick cross sections with the use of a diamond wafering saw cooled with phosphate-buffered saline (PBS). The bone marrow was removed manually, and the samples were immediately immersion-fixed. It is widely assumed that a major component of the pericellular material surrounding osteocyte processes is proteoglycan (PG) (Sauren et al., 1992). These molecules are notoriously difficult to fix for microscopy studies, hence an improved technique in which the PG can be preserved is required. Hunziker et al. (1982) showed that the addition of ruthenium III hexamine trichloride (RHT) to the primary aldehyde fixatives could greatly improve the preservation of PGs in cartilage. This also resulted in improved preservation of chondrocytes, since the charge density of the tissue was maintained (Hunziker et al., 1982). The principal advantage of using ruthenium-containing fixatives in cartilage is that they avoid the creation of a pericellular lacunar space by preserving the interconnected nature of the matrix PGs, and the integrity of the latter with the chondrocyte plasma membrane and matrix vesicle membranes. With RHT, the fixatives are able to penetrate tissue blocks to a greater depth and in a more homogenous manner than is achievable with ruthenium red only. Thus, in the current ultrastructural studies, we combined RHT with standard fixative procedures to assess whether this combination would provide new information on the PG structure surrounding the osteocytic process.

The samples were fixed for 24 hr in one of the following four groups of fixatives: 1) group G: primary fixation media with glutaraldehyde only (2% glutaraldehyde in 0.05 M cacodylate buffer at 7.4 pH); 2) group GR: primary fixation media with glutaraldehyde and RHT (2% glutaraldehyde in 0.05 M cacodylate buffer at 7.4 pH containing 0.7% RHT); 3) group GP: primary fixation media with glutaraldehyde and paraformaldehyde (2% glutaraldehyde and 4% paraformaldehyde in 0.05 M cacodylate buffer at 7.4 pH); and 4) group GPR: primary fixation media with glutaraldehyde, paraformaldehyde, and RHT (2% glutaraldehyde and 4% paraformaldehyde in 0.05 M cacodylate buffer with 0.7% RHT at 7.4 pH).

The specimens were then decalcified with 10% EDTA in 0.1 M Tris-HCL buffer for 2 weeks. Prior to postfixation, the tissue blocks were washed for 3 × 5 min in the Tris buffer. Postfixation was then carried out in 1% osmium

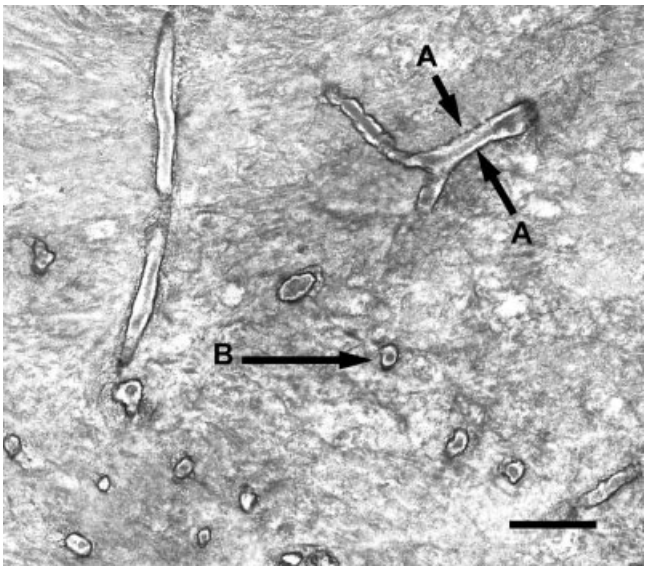

Fig. 1. Electron photomicrograph showing several longitudinal and transverse cross sections of osteocyte processes. The central positioning of the processes in the canaliculi is clearly visible. A: Longitudinal section of a canaliculus with a cell process at its center. The black line is the canalicular wall. B: Transverse cross section of a canaliculus with a cell process at its center. The black line along the circle is the canalicular wall. Bar = 1 μm.

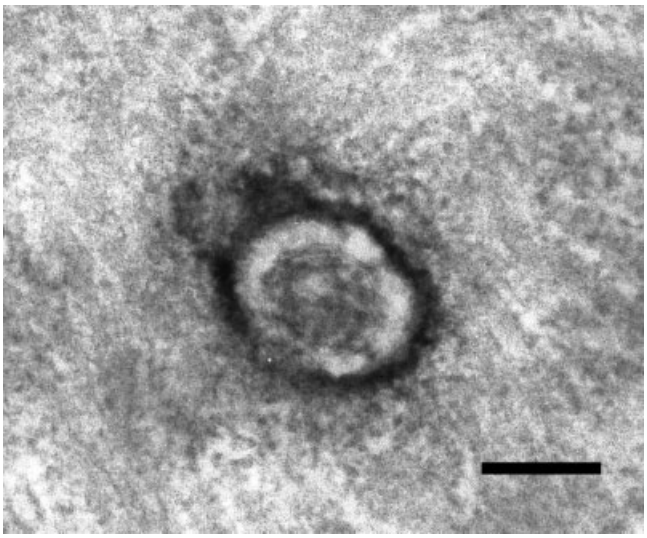

Fig. 2. Electron photomicrograph showing the cross section of an osteocyte process, with a pericellular matrix surrounding the osteocyte process. GPR-fixed. Bar = 100 nm.

tetroxide in Tris buffer. During all of the processing steps, the RHT concentration and identical pH were maintained. The specimens were then washed in PBS, dehydrated in graded ethanols, and infiltrated for 1 week in a mixture of epon and propylene oxide (Weinger and Holtrop, 1974). The specimens were embedded in epon with the longitudinal axis of the bone parallel to the sectioning surface so that optimal registration of cross or longitudinal sections of osteocyte processes could be obtained. Ultrathin sections were cut with a diamond knife and stained with a saturated solution of uranyl acetate in 50% ethanol followed by 0.2% lead citrate. The sections were placed on Parlodion-coated 200-mesh copper grids, and viewed with a Philips EM 300 electron microscope.

All ultrastructural measurements were made directly from micrographs and performed by a single investigator. The data are shown as mean ± standard deviation.

RESULTS

Comparison of Fixatives

The best preservation was obtained when the three fixatives were employed together (group GPR). With this group of fixatives, the pericellular matrix and the osteocyte process itself were well preserved. Within the pericellular space surrounding the process (Figs. 1 and 2), transversely oriented fiber-like elements were observed extending from the process membrane to the canalicular wall. Microfilaments within the process were also clearly observed. Fixation was not as good when RHT was combined with glutaraldehyde alone: the pericellular matrix was less well preserved, and the intracellular structure was lost. When the glutaraldehyde was combined with the highly-penetrating fixative (paraformaldehyde) but without RHT, cellular structures, such as the cell membrane and the cytoskeleton, were well preserved, but the pericellular matrix was lost. Finally, glutaraldehyde alone was unsuitable.

Pericellular Space, and Dimensions of the Osteocytic Processes, the Canaliculi, and the Pericellular Space

In both longitudinal and transverse sections, the osteocyte processes were always observed surrounded by a pericellular space and symmetrically centered within the canaliculi (Fig. 1). The presence of a uniformly distributed pericellular matrix surrounding the osteocyte process and filling the entire space suggests that the pericellular space is indeed a real space and not a shrinkage artifact. An enlarged cross section of an osteocyte process is shown in Figure 2, group GPR. One can see that the pericellular matrix surrounds the process, and the canalicular wall is darkly stained by the RHT. If the pericellular space resulted from shrinkage, no matrix would be observed in this space. Measurements of the dimensions of the processes, the canaliculi, and the pericellular space were made on transverse sections of canaliculi. We measured the diameters of the osteocytic processes and the canaliculi directly from the cross sections of the canaliculi. The results are summarized in Figure 3. The osteocytic process diameters varied from 50 to 410 nm, and the canalicular diameters varied from 80 to 710 nm. The measured average diameter of the canaliculi was 259 ± 129 nm. The reason for the variability of these values is not clear. One possibility is that the dimensions of the canaliculi and process are position-dependent. We found that the process and the canaliculi are always wide when they are close to the cell body. Thus, we speculate that the position of the measurement taken may have contributed to the variation in the dimension of the structures. The average diameter of the cell process was 104 ± 69 nm. Using these data, the average width of the pericellular annulus or space around the osteocyte process was 78 ± 38 nm.

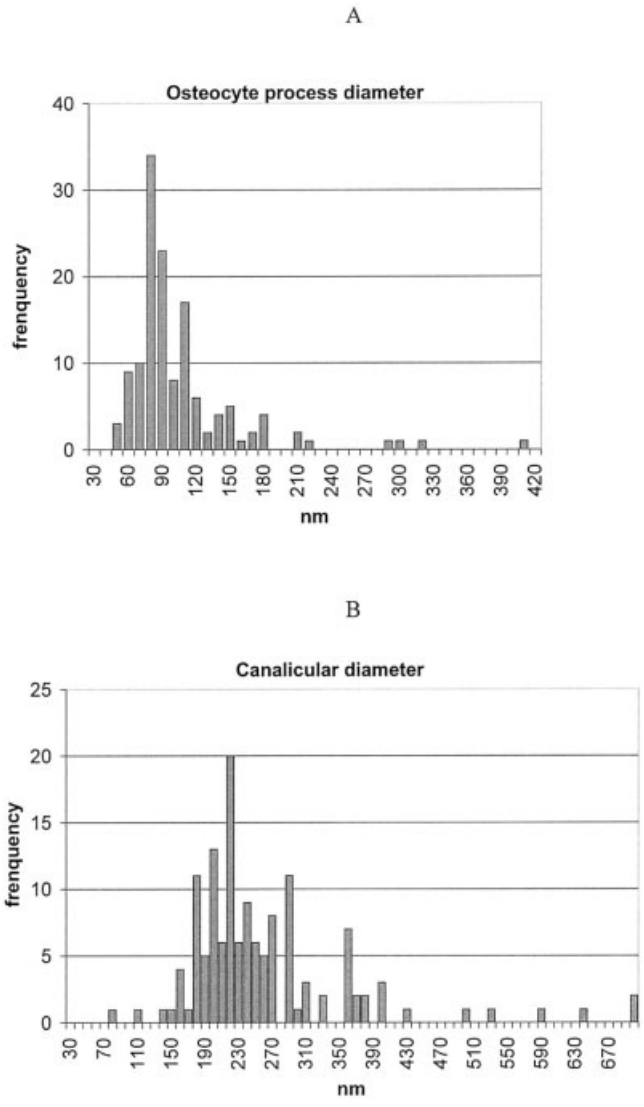

Fig. 3. Measurements of osteocyte process and canalicular diameters: (A) process diameter, n = 137; (B) canalicular diameter, n = 137.

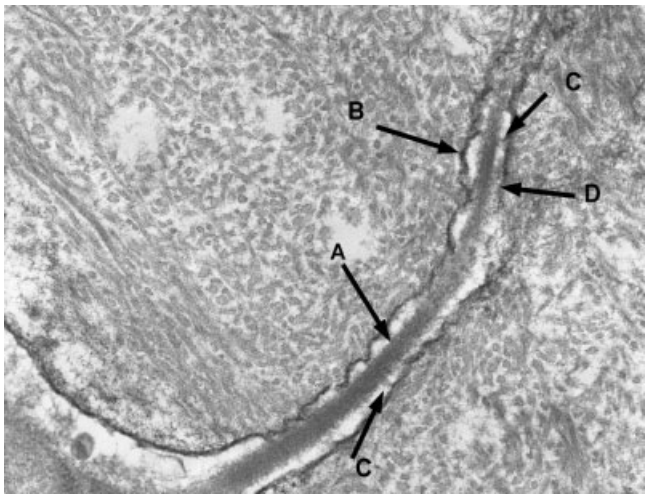

Fig. 4. Electron photomicrograph of a longitudinal section through an osteocyte process: (A) cell process, (B) canalicular wall, (C) transverse elements connecting the process to the canalicular wall, and (D) pericellular matrix filling the annular space. GPR-fixed. Bar = 200 nm.

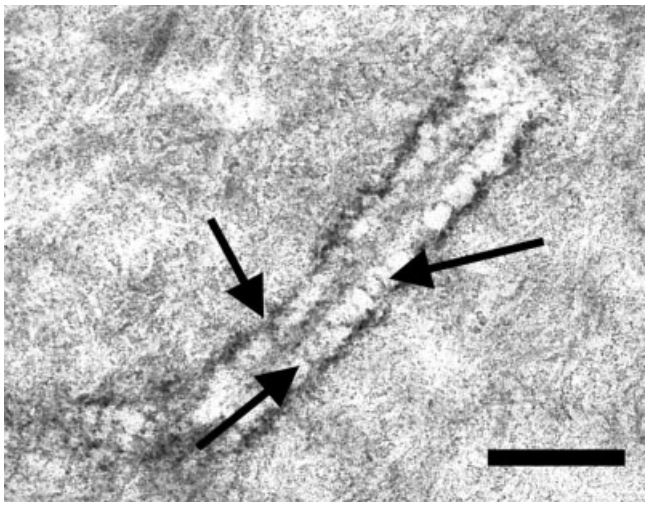

Fig. 5. Electron photomicrograph showing the longitudinal section of an osteocyte process. Numerous transverse elements (arrows) can be seen extending from the cell process to the bony wall. GPR-fixed. Bar = 300 nm.

Transverse Tethering Elements and the Spacing Between Them

Transverse elements were found spanning the entire pericellular space from the osteocyte process membrane to the canalicular wall. They were visible in both transverse and longitudinal sections. These elements were dense and arranged in a periodic fashion (Figs. 4 and 5). Measurements of the spacing between these transverse elements were made on both longitudinal and transverse sections of canaliculi. The transverse elements can be clearly seen in the pericellular space surrounding the osteocytic process. The number of transverse elements was counted. We estimated the spacing between the transverse elements by dividing the length or cell membrane perimeter in the section by the number of transverse elements contained in the portion of the longitudinal/transverse section. The results are summarized in Figure 6. The spacing varies from 12 to 76 nm in the longitudinal direction, and from 20 to 115 nm in the cross-sectional direction. The mean value for this spacing was 38 ± 21 nm for longitudinal sections, and 41 ± 24 nm for transverse sections. There was no significant difference in the spacing in the longitudinal and transverse directions (ANOVA, $P > 0.05$). Exact measurements of transverse element spacing cannot be obtained from the current studies, as these measurements include some volume projection effects due to the thickness of the section. However, one can estimate a section-thickness correction, and correct the counts assuming that the distances between the transverse elements are the same in both the longitudinal and transverse sections (Weibel, 1980). With this correction, the average spacing is increased by about 20%. There is great variation in the

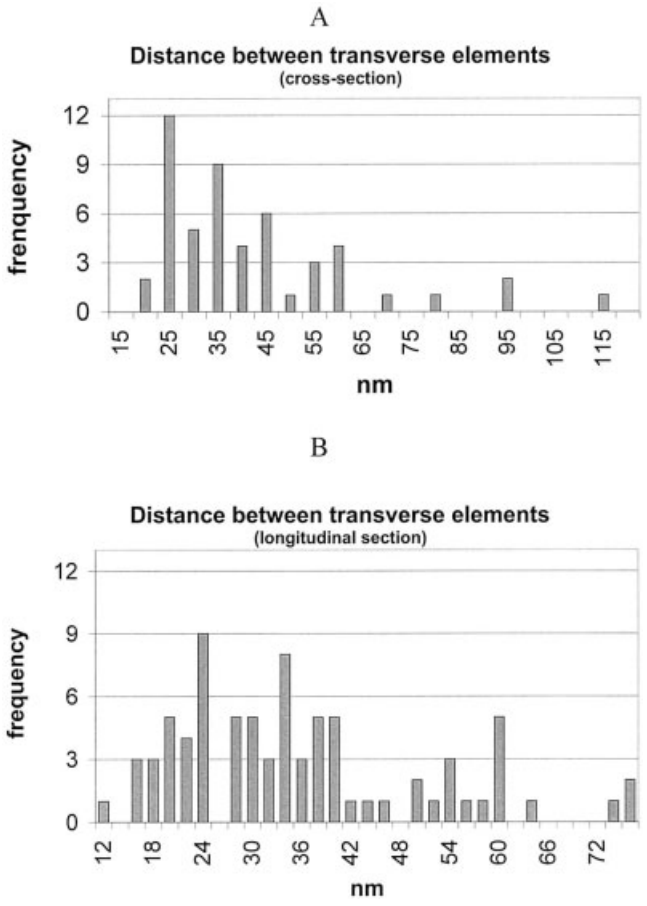

Fig. 6. Measurements of spacing between transverse elements in the pericellular space surrounding the osteocytic process: (A) cross section, n = 53; (B) longitudinal section, n = 84.

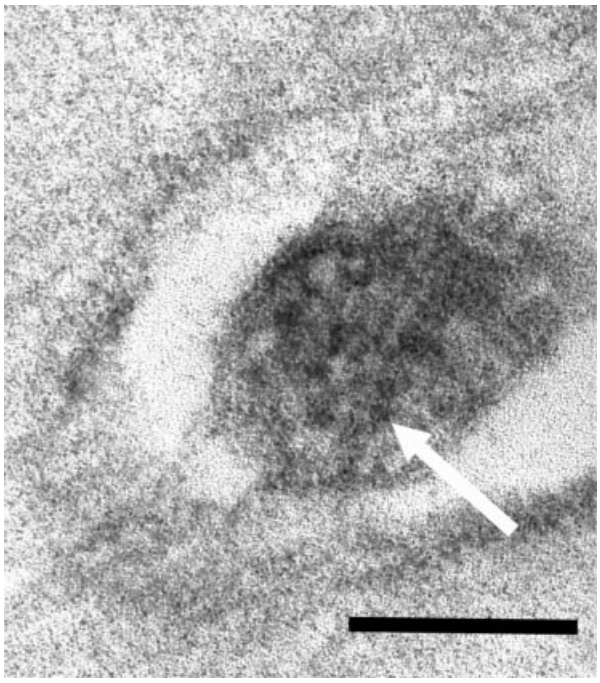

Fig. 7. Electron photomicrograph showing a cross section of an osteocyte process. Darkened circular spots (see arrow) are cross sections of cytoskeletal filaments ~6–8 nm in diameter, consistent with the size of actin filaments. Bar = 100 nm.

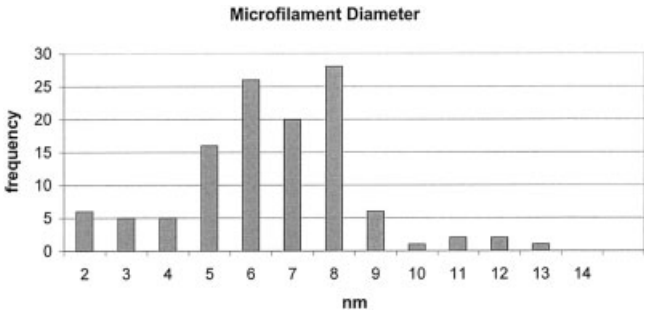

Fig. 8. Measurements of the diameter of the microfilaments in the osteocyte processes. n = 127.

measurements of the spacing between the transverse elements. However, in the microscopic pictures of each process we observed, the transverse elements were always regularly spaced. Therefore, we speculate that this variability may be due to volume projection effects caused by the section thickness, or to the staining technique used (i.e., some of the transverse elements did not stain strongly enough for visual detection).

Microfilaments in Cell Processes, and Spacing Between the Filaments

Microfilaments were observed in the osteocyte process in both longitudinal sections (where they appear as axial filaments (Fig. 4)) and transverse sections (where they appear as small darker spots inside the process (Figs. 2 and 7)). The diameters of the microfilaments within the osteocyte process were measured directly from electron photomicrographs. The results are shown in Figure 8. The diameters varied from 2 to 13 nm, and the mean value of the measurements for the microfilament diameters was 7.3 nm. The spacing between the axial microfilaments was evaluated from transverse sections of osteocytic processes. The diameters of the osteocytic processes were measured, and the cross-sectional areas were calculated based on these diameters, assuming a circular profile. The number of the actin filaments in each cross section was counted. By dividing the cross-sectional area of the osteocytic process by the number of the microfilaments within the cross section, we obtained the average area surrounding each microfilament. The diameter of this effective circular area can be taken as the spacing between the microfilaments. We calculated the actual spacing by dividing the effective diameter by the corresponding magnification. The results are shown in Figure 9. The values varied from 20 to 80 nm, and the mean value of the measurements for the spacing between the microfilaments was 32 ± 14 nm.

DISCUSSION

These experimental studies confirm the existence of the fundamental microstructural features needed for strain

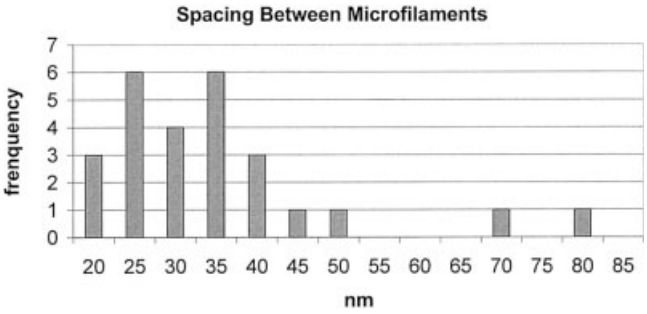

Fig. 9. Measurements of spacing between the microfilaments in the osteocyte processes. n = 27.

amplification to occur in loaded bone. In addition, these measurements for the essential structural dimensions are in reasonable agreement with the assumed parameter values in our theoretical model (You et al., 2001).

The ultrastructural features assumed in the theoretical model described by You et al. (2001) are 1) the existence of the pericellular space, 2) the presence of a space-filling pericellular matrix, 3) the existence of transverse tethering elements in the pericellular space, and 4) the presence of a space-filling actin filament bundle in the cell process. The essential geometrical parameters required in the theoretical model are 1) the dimensions of the canaliculi, the osteocytic processes, and the pericellular space; 2) the spacing between the transverse tethering elements; and 3) the spacing between the axially-oriented microfilaments. These assumptions and parameter values are discussed below.

While most researchers believe there is a pericellular space surrounding the osteocytic process in the canaliculus, there is no complete agreement on this issue. Many theoretical models involving fluid flow in the lacuno-canalicular system have been constructed based on the assumption that the cell process is surrounded by a pericellular space (Salzstein et al., 1987; Weinbaum et al., 1994; Zeng et al., 1994; Cowin et al., 1995; Wang et al., 1999, 2000). Indirect evidence was obtained from experimental studies (Knothe Tate et al., 1998, 2001; Knothe Tate and Knothe, 2000; Wang et al., 2004) in which the penetration of different-sized (<10 nm) molecular tracers into the lacuno-canalicular system was observed after the tracer was injected into an animal's vascular system.

However, some investigators have expressed concern as to whether the pericellular spaces observed in bone are artifacts resulting from shrinkage due to fixation (Wassermann and Yaeger, 1965; Weinger and Holtrop, 1974; Shapiro et al., 1995). These previous studies were performed on osteocytes in immature bone that had only recently been entombed in the matrix and were thus much larger than mature osteocytes, and appeared to be more closely applied to the bony lacunar and canalicular walls. Since all of the previous studies regarding the pericellular space were conducted on young animals, the question also remained as to whether this space exists in mature animals.

In the current studies, the existence of the pericellular space surrounding osteocytes is clearly demonstrated in mature animal bone. The pericellular space observed in our study appears to exist in the living state and is not a shrinkage artifact. If the space was an artifact due to shrinkage, it would appear empty on the micrographs. In our study, the pericellular space was always filled with matrix, which was particularly well preserved by a combination of highly-penetrating fixative (GP) and cationic fixative (RHT). The addition of RHT preserves the PG matrix content of the pericellular space. This observation strongly supports the view that the PGs are a major constituent of the pericellular matrix (Hunziker et al., 1982). The existence of the pericellular space is an essential assumption in all theoretical models involving fluid flow in the lacuno-canalicular system of bone.

These studies clearly demonstrate for the first time the existence of the transverse tethering elements that connect the osteocytic process to the canalicular wall. Both the transverse and longitudinal sections of the canaliculi indicated that osteocytic processes are nearly always located in the center of the canaliculi. If there were no connections between the osteocytic processes and the canalicular wall, the processes would be located randomly inside the canaliculi instead of always being centered within the canaliculi. This strongly suggests that the osteocytic processes are tethered in their central position, since the canaliculi are often curved, as shown in Figure 4, and the cell processes still centrally adjust to this curvature. In the current studies, the transverse tethering elements can be clearly observed in both the longitudinal and transverse sections of the canaliculi. Prior to the present study, the existence of transverse elements was mentioned only anecdotally by Shapiro et al. (1995). You et al. (2001) inferred the existence of transverse tethering elements from a functional viewpoint based on the ubiquitous centering of the cell processes, without direct supporting histological evidence for the existence of the tethering filaments.

An important observation with respect to the theoretical model of You et al. (2001) is that the transverse fibers span the entire pericellular space, and thus provide direct linkage of the osteocyte process with the canalicular wall. With this structure, the drag forces exerted on the pericellular matrix can be transmitted by the transverse tethering elements to the actin filament bundle within the cell process, and induce cell deformations that are of sufficient magnitude to elicit an intracellular signaling response.

While our current studies indicate that the osteocytes are tethered to the canalicular wall by means of the transverse elements, the identity of these transverse elements and their connections to the intracellular structure remains unclear. Possible candidates for the attachment molecules for this tethering include CD44, laminin, and various integrins. CD44, which is a cell surface receptor of hyaluronic acid (HA), has been found on the surface of osteocytes (Hughes et al., 1994; Nakamura et al., 1995; Jamal and Aubin, 1996; Nakamura and Ozawa, 1996; Noonan et al., 1996). Specifically, Noonan et al. (1996) labeled both HA and CD44 along the canaliculi.

The present study is the first to observe the transverse elements with sufficient clarity to measure this spacing quantitatively. The length of these filaments is approximately 80 nm, which is also the width of the pericellular space surrounding the cell process. The average measured spacing is 38 nm in a longitudinal section, and 41 nm in a cross section. Since the spacing of PG binding sites along HA has been reported to be on the order of 30–40 nm (Lodish, 1999; Hascall, 2000; McDonald and Hascall,

TABLE 1A. Estimated values for the diameters of the canaliculi and the osteocyte processes taken from EM micrographs in the literature

Bone	Canalicular diameter[a] (nm)	Osteocyte process diameter[b] (nm)	Width of pericellular annulus[c] (nm)	References
Human tibia, various ages	≈700			Figs. 6, 7 (Marotti et al., 1979)
15 day old chick	≈400	≈200	≈100	Fig. 3.22 (Palumbo, 1986)
New born rabbit	≈125			Fig. 1 (Palumbo et al., 1990a)
New born rabbit	≈200			Fig. 10 (Palumbo et al., 1990b)
Human compact bone	≈100			Fig. 19a (Marotti, 1996)
Human compact bone	≈200			Fig. 19b (Marotti, 1996)
Human compact bone	≈300			Fig. 20 (Marotti, 1996)

[a]Estimated value of the canalicular diameter.
[b]Estimated value of the osteocyte process diameter.
[c]Width is determined by subtracting the osteocyte process diameter from the canalicular diameter and dividing by two.

2002), which is nearly the same as the average spacing of the tethering filaments, it is reasonable to speculate that the HA is attached along the membrane by the extracellular loops of the CD44, and that the PGs are the transverse elements that span the pericellular space. A possible candidate for the adhesion molecule at the canalicular wall is laminin.

A number of studies have demonstrated the presence of microfilament bundles within the osteocytic process in young animals (Weinger and Holtrop, 1974; Holtrop, 1975; King and Holtrop, 1975). In 1998, an in vitro immunohistochemical study by Tanaka-Kamioka et al. (1998) showed the existence of an actin filament bundle in the osteocytic process, with fimbrin and α-actinin serving as linker molecules between the actin filaments. However, questions remained as to why this extensive cytoskeletal structure is needed, and whether it exists in mature osteocytes. In their mechanotransduction model, You et al. (2001) concluded that a significantly stiffer cytoskeletal structure (compared to the cell body) must exist inside the osteocyte process to balance the strong fluid flow-induced drag force transmitted from the pericellular matrix to the cytoskeleton, in order for reasonable deformations of the cell process to be obtained. Our observations of microfilaments inside the process confirm the existence of an axial filament bundle structure in mature osteocytes. The microfilaments we measured were 7.3 nm in diameter, which is typical of the diameter of F-actin. However, an immunohistochemical study is needed before a definitive identification can be made.

With regard to the spacing between the axial microfilaments in the cell process, there is no previous mention of this parameter in the literature. The only related data we could find were regarding similar structures in the microvilli in the kidney and intestine, and in the hair cells of the inner ear (Weinbaum et al., 2001). All three of these structures have axial actin filament bundles as their central cytoskeleton, with fimbrin, villin, or actinin as the common linker molecules between the actin filaments. The spacing between the actin filaments varies from 12 nm in stereocilia to 25 nm in kidney microvilli. Both of these values are smaller than the typical 32-nm spacing we measured in the osteocytic process. However, this estimate of microfilament spacing neglects the facts that the actin filament bundle is confined to the central region of the process, and there are no microfilaments in the immediate vicinity of the membrane. This is consistent with electron micrographic studies of intestinal microvilli that demonstrated a filament-free region of approximately 20-nm thickness surrounding the actin filament bundle. In intestinal microvilli, this region contains a helical spiral of brush border myosin I that forms a cortex on which the cell membrane rests (Mooseker and Tilney, 1975). Therefore, given that the actin filaments are uniformly distributed only in the center part of the process, the spacing between the filaments should be calculated as the center area (occupied by actin filaments), instead of the entire area of the process, divided by the number of actin filaments, which will lead to the value of the spacing of the actin filaments in the process be reduced to 19.7 nm. The 25-nm spacing assumed by You et al. (2001) in their model is therefore a reasonable estimate. With our current staining technique, we were unable to assess the three-dimensional arrangement of the actin filaments and their linker molecules (fimbrin and α-actinin).

The essential geometric parameters in all of the theoretical models that involve fluid flow in the lacuno-canalicular porosity are the dimensions of the canaliculi, the osteocytic processes, and the pericellular space surrounding the osteocytic process. These parameters greatly influence the results of calculations (e.g., the shear stress on the osteocyte process membrane, and the streaming potential). Although many ultrastructural studies have shown micrographs of osteocyte processes in canaliculi, no systematic quantitative study has been conducted on these parameters. Moreover, there is a lack of agreement between researchers on the reported values of these parameters. For the purpose of comparison, we examined canaliculi and processes taken from the literature, using either published measurements or our own measurements derived from published photographs (Table 1). Given that the fixation techniques exploited in previous studies were different from ours, one should exercise caution when interpreting the measurements from these studies in comparison with the current results. From the data in the literature (Table 1), it appears that the diameters of cell processes and canaliculi vary depending on the species and the age of the animals. The values of these parameters were also predicted in some theoretical models from a functional viewpoint. In presenting their theoretical model Kufahl and Saha (1990), pointed out that the canalicular diameter should fall within the range of 100–800

TABLE 1B. Summary of the values of the dimensions of the canaliculi, the osteocyte processes, and the pericellular space appearing in the literature

Canalicular (diam.)	Process (diam.)	Pericellular space (width)	References
85–100 nm		14–100 nm	Cooper et al., 1966
150–550 nm			Marotti, 1990
150–550 nm	80–100 nm	25–235 nm	Marotti et al., 1990
150–200 nm			Figs. 11, 13 (Steflik et al., 1994)

nm. Their calculations suggest that the canalicular diameter should be ~200 nm to satisfy metabolic requirements. However, their model of the canaliculus neglected the presence of the cell process.

From the above analysis, one can conclude that the size of the canaliculi and the osteocytic process may depend greatly on the species and the age of the animal. However, none of the previous studies were observational or quantitative. Therefore, we performed a detailed quantitative investigation of these geometric parameters in one animal species (adult mice). Additional studies are needed to examine the effects of animal age and species on these parameters.

To our knowledge, this is the first time that RHT has been utilized for the primary fixation of bone tissue. We found that in addition to improving fixation of the matrix in the pericellular space, RHT provides a very pronounced staining of the canalicular wall, which appears as a condensed dark region. We believe this dense region is due to the aggregation of the PGs along the canalicular wall, consistent with the crystalline staining of GAGs at this surface that has been observed with the use of cuprolinic blue (Sauren et al., 1992). The width of the fluid annulus surrounding the cell process would be nearly the same in traditional and RHT staining methods if the thickness of this condensed black line were taken into account. The average measured canalicular diameter was 259 nm. The average measured process diameter was 104 nm. From these two values, one can calculate the width of the pericellular space, which is 78 nm. Comparing these results with the corresponding parameter values assumed by You et al. (2001) (200 nm for the canalicular diameter, 100 nm for the process diameter, and 50 nm for the pericellular space), and considering the sensitivity analysis shown in Table 1 in You et al. (2001), one can conclude that the parameter values used in the theoretical model are reasonable, although the assumed width of the pericellular space is on the low side.

In conclusion, the current study reveals a complex ultrastructural architecture within osteocyte processes and, perhaps more significantly, the pericellular space surrounding the process. These observations demonstrate unequivocally that the osteocyte cell process is not a free-floating structure within the canaliculi, but rather is tethered to the canalicular wall. The existence of this structured pericellular matrix is consistent with that postulated by You et al. (2001) to give rise to drag and consequent hoop strains when the transverse tethering elements are placed in tension due to flow-induced drag forces on the pericellular matrix, resulting in an amplification of membrane strains by an order of magnitude. These observations show that osteocytes are contained within a pericellular matrix, which by virtue of its structure can affect the way that osteocytes experience their mechanical environment. That is, osteocyte processes and their surrounding matrix possess a range of ultrastructural elements, which, according to our previous theoretical model (You et al., 2001), should allow for a dramatic amplification of cellular-level strains.

ACKNOWLEDGMENTS

The microscopy in this study was performed at the Mount Sinai School of Medicine-Microscopy Shared Research Facility, which is supported in part by funding from an NIH-NCI shared resources grant (1 R24 CA095823-01). This work was completed in partial fulfillment of the requirements for a doctoral degree by Lidan You, from the City University of New York. We thank Dr. Scott Henderson for his guidance and advice throughout this research, and Ms. Valerie Williams for expert technical assistance with the electron microscopy studies.

LITERATURE CITED

Bentolila V, Boyce TM, Fyhrie DP, Drumb R, Skerry TM, Schaffler MB. 1998. Intracortical remodeling in adult rat long bones after fatigue loading. Bone 23:275–281.

Cooper RR, Milgram JW, Robinson RA. 1966. Morphology of the osteon. An electron microscopic study. J Bone Joint Surg Am 48: 1239–1271.

Cowin SC, Weinbaum S, Zeng Y. 1995. A case for bone canaliculi as the anatomical site of strain generated potentials. J Biomech 28: 1281–1297.

Fritton SP, McLeod KJ, Rubin CT. 2000. Quantifying the strain history of bone: spatial uniformity and self-similarity of low-magnitude strains. J Biomech 33:317–325.

Hascall VC. 2000. Hyaluronan, a common thread. Glycoconjugate J 17:607–616.

Holtrop ME. 1975. The ultrastructure of bone. Ann Clin Lab Sci 5:264–271.

Hughes DE, Salter DM, Simpson R. 1994. CD44 expression in human bone: a novel marker of osteocytic differentiation. J Bone Miner Res 9:39–44.

Hunziker EB, Herrmann W, Schenk RK. 1982. Improved cartilage fixation by ruthenium hexammine trichloride (RHT). A prerequisite for morphometry in growth cartilage. J Ultrastruct Res 81:1–12.

Jamal HH, Aubin JE. 1996. CD44 expression in fetal rat bone: in vivo and in vitro analysis. Exp Cell Res 223:467–477.

King GJ, Holtrop ME. 1975. Actin-like filaments in bone cells of cultured mouse calvaria as demonstrated by binding to heavy meromyosin. J Cell Biol 66:445–451.

Knothe Tate ML, Knothe U, Niederer P. 1998. Experimental elucidation of mechanical load-induced fluid flow and its potential role in bone metabolism and functional adaptation. Am J Med Sci 316: 189–195.

Knothe Tate ML, Knothe U. 2000. An ex vivo model to study transport processes and fluid flow in loaded bone. J Biomech 33:247–254.

Knothe Tate ML, Tami A, Nasser P, Steck R, Schaffler M. 2001. Permeability characteristics of different molecular tracers in loaded

and unloaded bone. In: Proceedings of the 47th Annual Meeting of the Orthopaedic Research Society, San Francisco. p 0138.
Kufahl RH, Saha S. 1990. A theoretical model for stress-generated fluid flow in the canaliculi-lacunae network in bone tissue. J Biomech 23:171–180.
Lodish H, Berk A, Zipursky L, Matsudaira P, Baltimore D, Darnell J. 1999. Molecular cell biology. 4th ed. New York: W.H. Freeman and Company.
Marotti G, Delrio N, Marotti F, Fadda M. 1979. Quantitative analysis of the bone destroying activity of osteocytes and osteoclasts in experimental disuse osteoporosis. Ital J Orthop Traumatol 5:225–240.
Marotti G. 1990. Ultrastructure of skeletal tissue. Boston: Kluwer Academic Publisher.
Marotti G, Cane V, Palazzini S, Palumbo C. 1990. Structure-function relationships in the osteocyte. Ital J Miner Electrolyte Metab 4:93–106.
Marotti G. 1996. The structure of bone tissues and the cellular control of their deposition. Ital J Anat Embryol 101:25–79.
McDonald J, Hascall VC. 2002. Hyaluronan minireview series. J Biol Chem 15;277:4575–4579.
Mooseker MS, Tilney LG. 1975. Organization of an actin filament-membrane complex. Filament polarity and membrane attachment in the microvilli of intestinal epithelial cells. J Cell Biol 67:725–743.
Nakamura H, Kenmotsu S, Sakai H, Ozawa H. 1995. Localization of CD44, the hyaluronate receptor, on the plasma membrane of osteocytes and osteoclasts in rat tibiae. Cell Tissue Res 280:225–233.
Nakamura H, Ozawa H. 1996. Immunolocalization of CD44 and the ERM family in bone cells of mouse tibiae. J Bone Miner Res 11: 1715–1722.
Noonan KJ, Stevens JW, Tammi R, Tammi M, Hernandez JA, Midura RJ. 1996. Spatial distribution of CD44 and hyaluronan in the proximal tibia of the growing rat. J Orthop Res 14:573–581.
Palumbo C. 1986. A three-dimensional ultrastructural study of osteoid-osteocytes in the tibia of chick embryos. Cell Tissue Res 246: 125–131.
Palumbo C, Palazzini S, Marotti G. 1990a. Morphological study of intercellular junctions during osteocyte differentiation. Bone 11: 401–406.
Palumbo C, Palazzini S, Zaffe D, Marotti G. 1990b. Osteocyte differentiation in the tibia of newborn rabbit: an ultrastructural study of the formation of cytoplasmic processes. Acta Anat 137:350–358.
Piekarski K, Munro M. 1977. Transport mechanism operating between blood supply and osteocytes in long bones. Nature 269:80–82.
Rubin CT, Lanyon LE. 1984. Regulation of bone formation by applied dynamic loads. J Bone Joint Surg Am 66:397–402.
Salzstein RA, Pollack SR, Mak AF, Petrov N. 1987. Electromechanical potentials in cortical bone—I. A continuum approach. J Biomech 20:261–270.
Sauren YM, Mieremet RH, Groot CG, Scherft JP. 1992. An electron microscopic study on the presence of proteoglycans in the mineralized matrix of rat and human compact lamellar bone. Anat Rec 232:36–44.
Shapiro F, Cahill C, Malatantis G, Nayak RC. 1995. Transmission electron microscopic demonstration of vimentin in rat osteoblast and osteocyte cell bodies and processes using the immunogold technique. Anat Rec 241:39–48.
Steflik DE, Sisk AL, Parr GR, Lake FT, Hanes PJ, Berkery DJ, Brewer P. 1994. Transmission electron and high-voltage electron microscopy of osteocyte cellular processes extending to the dental implant surface. J Biomed Mater Res 28:1095–1107.
Tanaka-Kamioka K, Kamioka H, Ris H, Lim SS. 1998. Osteocyte shape is dependent on actin filaments and osteocyte processes are unique actin-rich projections. J Bone Miner Res 13:1555–1568.
Wang L, Fritton SP, Cowin SC, Weinbaum S. 1999. Fluid pressure relaxation depends upon osteonal microstructure: modeling an oscillatory bending experiment. J Biomech 32:663–672.
Wang L, Cowin SC, Weinbaum S, Fritton SP. 2000. Modeling tracer transport in an osteon under cyclic loading. Ann Biomed Eng 28: 1200–1209.
Wang L, Ciani C, Doty SB, Fritton SP. 2004. Delineating bone's interstitial fluid pathway in vivo. Bone 34:499–509.
Wassermann F, Yaeger J. 1965. Fine structure of osteocyte capsule and of wall of lacunae in bone. Z Zellforsch Mikrosk Anat 67:636–652.
Weibel ER. 1980. Stereological methods. New York: Academic Press.
Weinbaum S, Cowin SC, Zeng Y. 1994. A model for the excitation of osteocytes by mechanical loading-induced bone fluid shear stresses. J Biomech 27:339–360.
Weinbaum S, Guo P, You L. 2001. A new view of mechanotransduction and strain amplification in cells with microvilli and cell processes. Biorheology 38:119–142.
Weinger JM, Holtrop ME. 1974. An ultrastructural study of bone cells: the occurrence of microtubules, microfilaments and tight junctions. Calcif Tissue Res 14:15–29.
You J, Yellowley CE, Donahue HJ, Zhang Y, Chen Q, Jacobs CR. 2000. Substrate deformation levels associated with routine physical activity are less stimulatory to bone cells relative to loading-induced oscillatory fluid flow. J Biomech Eng 122:387–393.
You L, Cowin SC, Schaffler MB, Weinbaum S. 2001. A model for strain amplification in the actin cytoskeleton of osteocytes due to fluid drag on pericellular matrix. J Biomech 34:1375–1386.
Zeng Y, Cowin SC, Weinbaum S. 1994. A fiber matrix model for fluid flow and streaming potentials in the canaliculi of an osteon. Ann Biomed Eng 22:280–292.